AIP | Applied Physics Letters

Observation of the inverse spin Hall effect in ZnO thin films: An all-electrical approach to spin injection and detection

Megan C. Prestgard and Ashutosh Tiwari

Citation: Applied Physics Letters **104**, 122402 (2014); doi: 10.1063/1.4869117
View online: http://dx.doi.org/10.1063/1.4869117
View Table of Contents: http://scitation.aip.org/content/aip/journal/apl/104/12?ver=pdfcov
Published by the AIP Publishing

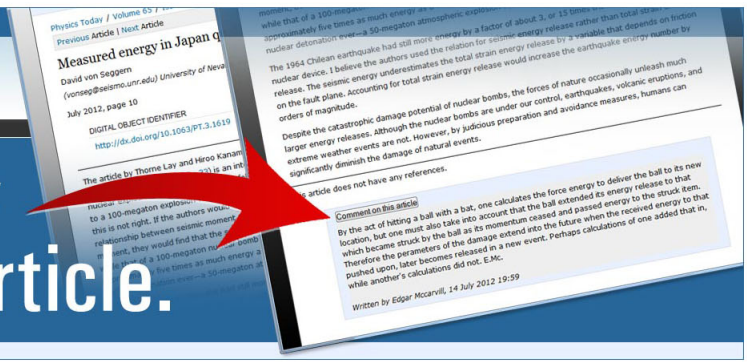

Observation of the inverse spin Hall effect in ZnO thin films: An all-electrical approach to spin injection and detection

Megan C. Prestgard and Ashutosh Tiwari[a)]
Nanostructured Materials Research Laboratory, Department of Materials Science and Engineering, University of Utah, Salt Lake City, Utah 84112, USA

(Received 16 February 2014; accepted 6 March 2014; published online 24 March 2014)

The inverse spin Hall effect (ISHE) is a newly discovered, quantum mechanical phenomenon where an applied spin current results in the generation of an electrical voltage in the transverse direction. It is anticipated that the ISHE can provide a more simple way of measuring spin currents in spintronic devices. The ISHE was first observed in noble metals that exhibit strong spin-orbit coupling. However, recently, the ISHE has been detected in conventional semiconductors (such as Si and Ge), which possess weak spin-orbit coupling. This suggests that large-spin orbit coupling is not a requirement for observing the ISHE. In this paper, we are reporting the observation of the ISHE in an alternative semiconductor material, zinc oxide (ZnO) using all-electrical means. In our study, we found that when a spin-polarized current is injected into the ZnO film from a NiFe ferromagnetic injector via an MgO tunnel barrier layer, a voltage transverse to both the direction of the current as well as its spin-polarization is generated in the ZnO layer. The polarity of this voltage signal was found to flip on reversing the direction of the injected current as well as on reversing the polarization of the current, consistent with the predictions of the ISHE process. Through careful analysis of the ISHE data, we determined a spin-Hall angle of approximately 1.651×10^{-2} for ZnO, which is two orders of magnitude higher than that of silicon. Observation of a detectable room-temperature ISHE signal in ZnO via electrical injection and detection is a groundbreaking step that opens a path towards achieving transparent spin detectors for next-generation spintronic device technology. © *2014 AIP Publishing LLC*. [http://dx.doi.org/10.1063/1.4869117]

As one of the most extensively studied semiconductor systems, zinc oxide and its derivatives have become increasingly prevalent in everyday technologies. The interest surrounding the ZnO system stems from its highly desirable and unique material properties. Specifically, ZnO has both a large bandgap of 3.37 eV and also a relatively high conductivity that can be easily tuned through simple material modifications.[1–3] In addition, and perhaps of most interest, are the optical properties of ZnO, namely, its transparency and large exciton binding energy (60 meV).[2,3] These traits have resulted in the exploration and use of ZnO for room temperature lasing and optoelectronic applications.[4–6] The versatile properties and numerous applications of ZnO give it both the potential to continue to satisfy current material needs as well as the capacity to provide a suitable framework for the future development of new and essential technologies. One such area that stands to benefit from this is the current electronics industry.

To this point, electronic devices, particularly transistors, have continued to miniaturize directly according to the prediction now known as Moore's law.[7,8] However, as devices approach the nanometer scale, adverse effects resulting from quantum confinement limitations will soon dominate and thus greatly hinder any further miniaturization of electronic devices.[9] This impending failure of Moore's law has led researchers to begin focusing on using alternative technologies to further device capabilities.[10,11] Included in these alternative technologies are spintronic devices. Spintronic devices already constitute a significant part of the electronics industry, particularly in the form of magnetic read-heads and magnetic-RAMs.[12,13] However, these devices are based on all-metallic constituents. In order to advance spintronic technology further, it is important to develop all-semiconductor-based spintronic devices where the transport, the manipulation, and the detection of spin-polarized electrons can be achieved via semiconductors themselves.[13–16] In the past, significant research efforts have been focused on semiconductor-based spintronics and a good understanding has been reached on the first two aspects, i.e., the transport and manipulation of spin-polarized carriers. However, there has still not been much progress in the field of semiconductor-based spin detectors. There has recently been a focus on examining spin-based effects and how these effects can be utilized for detecting spin-polarized carriers in spintronic devices.[17–20] One such effect is the spin Hall effect (SHE) and its counterpart, the inverse SHE (ISHE).

The spin-Hall effects refer to the coupling of spin and charge currents within a material. In the SHE, an applied charge current generates a transverse spin current.[21] Although the SHE is a well-known intrinsic material property, investigation into it has been limited by difficulties in the direct observation of spin currents. On the other hand, in the case of ISHE, an applied spin current results in the generation of an electrical voltage in the transverse direction.[22] This makes observation of the ISHE much more easily attainable than the SHE, as the electrical voltage can be measured simply via traditional electrical means.

In an ISHE process, the magnitude of the voltage generated, i.e., the ISHE signal, is directly proportional to the degree

a)Email: tiwari@eng.utah.edu

of spin-orbit coupling within a material.[23] For materials with large spin-orbit coupling, such as platinum, the transverse voltage generated can easily be used to detect spin accumulation. However, these materials cannot be integrated in traditional gate-type structures, which make them non-ideal for integration into current electronics. Because of this, it is necessary to discover semiconductor materials that show a strong ISHE signal. Recently, the ISHE has been reported in some common semiconductors, including Si and Ge, despite their having low spin-orbit coupling.[20,24] This is due to the fact that the ISHE signal is directly proportional to the product of the spin-orbit coupling and the resistivity of the material, which makes it possible to observe the ISHE in materials with low spin-orbit coupling if they are highly resistive.[20] In this paper, we are reporting the observation of an ISHE signal in ZnO using an all-electrical method and the subsequent calculation of its spin-orbit coupling and analysis of the potential of ZnO for dual optoelectronic-spintronic devices.

Thin films of ZnO were deposited using a pulsed laser deposition (PLD) technique under 10^{-4} Torr of O_2 pressure at 700 °C. For this, a highly dense ZnO target was ablated using a Lambda Physik COMPex Pro KrF excimer laser (wavelength = 248 nm, pulse width = 25 ns, and repetition rate = 10 Hz), giving approximately 200 nm thick films for a total of 8000 incident laser pulses. The films were characterized using a Philips X'Pert X-ray diffractometer to examine the crystal quality and orientation. Further characterization of the ZnO films was performed using UV-Vis spectroscopy (Lambda 950 model spectrometer). In order to characterize the overall electrical quality of the films, resistivity vs. temperature measurements were conducted in a closed-cycle cryostat over the temperature range of 15–300 K. On the well characterized ZnO films, an approximately 4 nm thick MgO tunnel barrier layer was deposited using PLD technique. The as-deposited layers were then patterned using a negative resist to form the desired "T" structure and etched using a dilute acid mixture (200 ml H_2O:1.5 ml H_3PO_4:0.1 ml HCl). The negative resist was then removed using acetone. Photolithography was then performed in order to pattern the substrate for the e-beam evaporation of the rectangular NiFe channel (Denton SJ20C).

The structural characterizations showed that the ZnO films were of high crystal quality, transparent, and possessed relatively high conductivities. As shown in Figure 1, the XRD results indicate that the ZnO thin films grown were highly c-axis aligned. The UV-Vis spectroscopy results proved that the ZnO thin films were transparent, thereby again confirming their high quality (see Figure 2(a)). The next characterization of the ZnO film was the measurement of electrical resistivity as a function of temperature. The results as presented in Figure 2(b) illustrate that the ZnO thin films were insulating, as was to be expected, but at the same time, they were of relatively low resistivity as compared to stoichiometric ZnO. Following these characterizations and the subsequent depositions of MgO and NiFe, the completed devices (illustrated in Figures 3(a) and 3(b)) were loaded into the ISHE electrical measurement system for testing.

The operation of the test device can be understood by examining the schematic shown in Figure 3(a). An in-plane magnetic field was first applied in order to magnetically

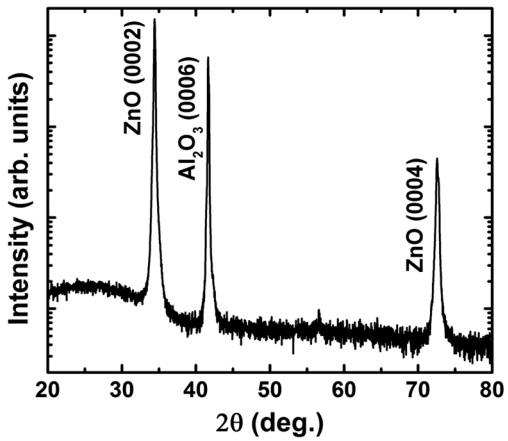

FIG. 1. X-ray diffraction characterization results of the ZnO thin films showing that the films grown were high quality and c-axis aligned.

polarize the spins in the NiFe film. The polarized carriers were then forced to move from point "a" in the NiFe to point "d" in the ZnO. This was done by applying a current between these two points. By passing a current between "a" and "d," the spin-polarized carriers in the NiFe first travel from point "a" to point "b." At point "b," the polarized carriers then tunnel from the NiFe through the MgO barrier into the ZnO (point "c"), as is shown in the cross-sectional view in Figure 3(b). Upon tunneling into the ZnO, the ISHE voltage signal develops between points c′ and c″. After this, the polarized

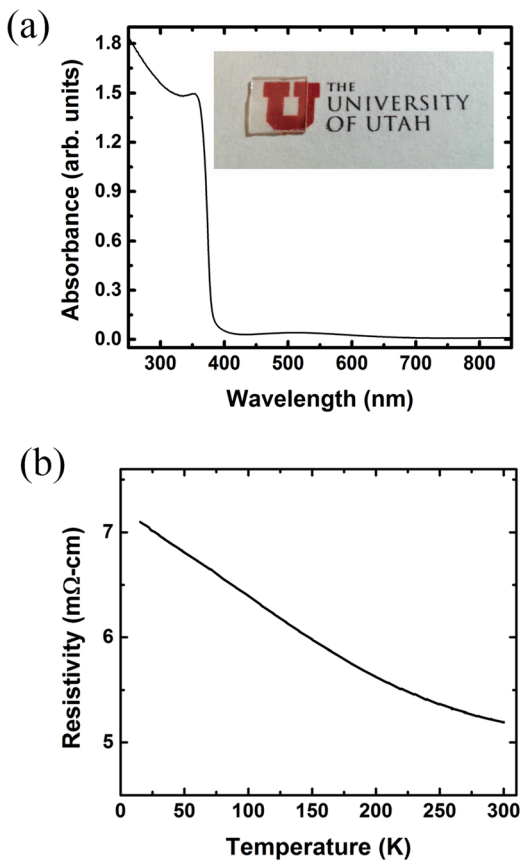

FIG. 2. (a) UV-Vis spectroscopy data for ZnO. The inset shows a photograph of the ZnO/Sapphire sample, illustrating its transparency. (b) Resistivity vs. temperature measurements showing that the sample is relatively conductive, as compared to stoichiometric ZnO, but is still semiconducting.

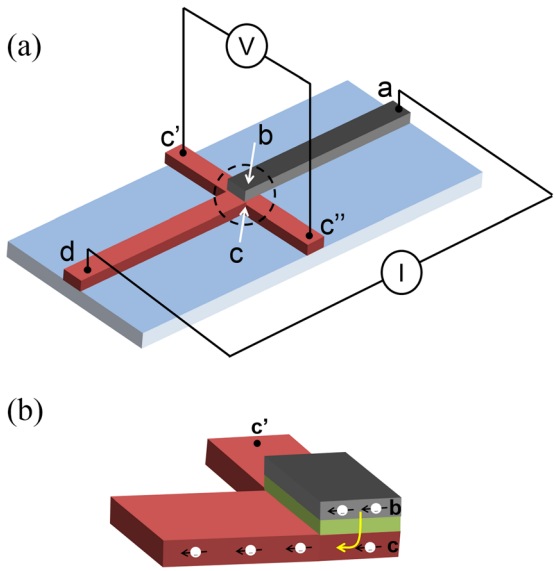

FIG. 3. Schematic illustrations of (a) the entire device structure and (b) a close-up of the ZnO/MgO/NiFe junction. The dashed circle in Figure 3(a) indicates the close-up region shown in part b, which illustrates the tunneling of polarized electrons from the NiFe into the ZnO via the MgO tunnel barrier. The red indicates ZnO, the blue is for the sapphire substrate, green for MgO, and gray for NiFe.

carriers continue traveling along the long ZnO channel until they reach point "d."

In order to probe the ISHE signal, the spin orientation of the injected carriers was modulated by changing the direction of the applied magnetic field. Specifically, the in-plane magnetic field was swept from +3 kG to −3 kG, during which time the voltage signal in the transverse channel was measured between points c′ and c″. As the direction of the magnetic field was switched, it was expected that the voltage should change from $+V_{ISHE}$ to $-V_{ISHE}$ upon changing the sign of the applied field. However, the actual signal (Figure 4) was found to be more complicated. This is because there is an additional contribution to the voltage which arises because of the magnetoresistance (MR) of the NiFe layer. Because of the finite size of the voltage contacts, it is impossible to have attained perfect alignment; thus, a MR contribution was added to the overall signal. However, when we examine the relative values of the voltages at the applied magnetic fields of +3 kG and −3 kG, the presence of the anticipated ISHE signal is evident. Specifically, as can be seen in Figure 4, there is a noticeable difference between the voltage at +3 kG and −3 kG, thereby indicating that the curve is not purely due to MR. As per the predictions of the ISHE theory, it was also expected that the ISHE signal should flip upon changing the sign of the spin injection current, which was verified via the +1 mA and −1 mA scans, Figures 4(a) and 4(b).

By subtracting out the MR contribution, the ISHE signal (Figure 5) was determined. Figures 5(a) and 5(b) show the ISHE signal for the positive and negative applied currents, respectively. The experimentally determined data are shown as solid points, with curves illustrating the anticipated behavior. The low-field data points, from approximately +0.5 kG to −0.5 kG, are shown with less color saturation than the high-field data. This is because the large MR background

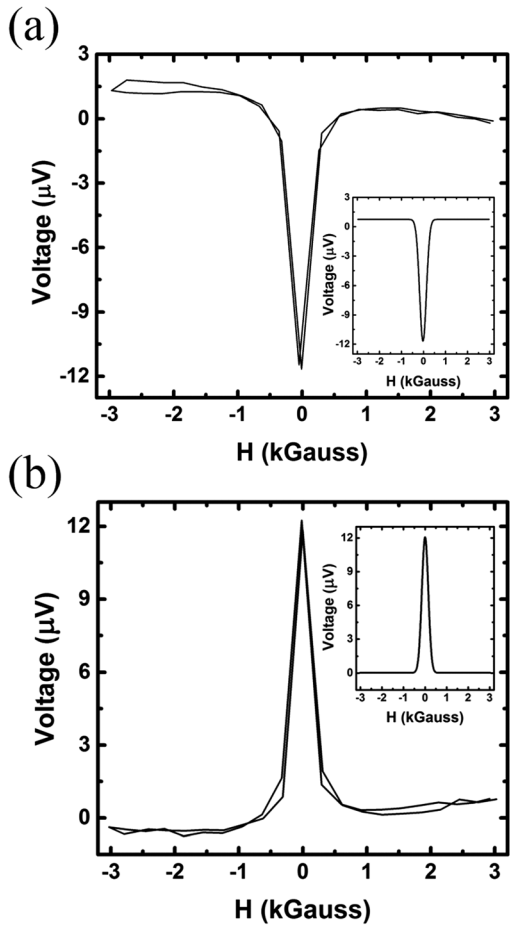

FIG. 4. The voltage between points c′ and c″ as a function of the applied, in-plane magnetic field. These data are a sum of both the background, NiFe magnetoresistance contribution, as well as the ZnO inverse spin Hall effect signal. Figures 4(a) and 4(b) indicate the scans at +1 mA applied current (from the NiFe to the ZnO) and −1 mA applied current (from the ZnO to the NiFe), respectively. The inset for each shows the background signal used for subtracting the MR contribution from the data.

that was present significantly limits detection of the ISHE signal within this low-field range. Thus, the color saturation in Figure 5 allows us to differentiate between the well-defined, high-field data and the uncertain, low-field data. From these plots, we are able to quantitatively determine the value of V_{ISHE}. As was explained previously, the V_{ISHE} is simply the average of the voltages at positive and negative 3 kG field values. From this, we then calculated the degree of spin-orbit coupling, specifically the spin-Hall angle, in the ZnO film. As can be seen in Eq. (1), the spin-Hall angle (θ_{SHE}) depends on the V_{ISHE}, the resistivity of the ZnO film (ρ_N), the injected spin current (I_s), and the width of the ZnO channel (w)

$$\theta_{SHE} = \frac{V_{ISHE}\ x\ w}{\rho_n\ x\ I_s}. \tag{1}$$

For this calculation, V_{ISHE} was determined to be approximately 0.6 μV from Figure 5. Resistivity was taken as 5.19 mΩ-cm, based on the aforementioned resistivity vs. temperature measurements (Figure 2(b)). The width of the channel was approximately 1 mm. The spin current, I_s, was taken as 0.7 mA, keeping into consideration the fact that NiFe can have a maximum attainable polarization of 70%.

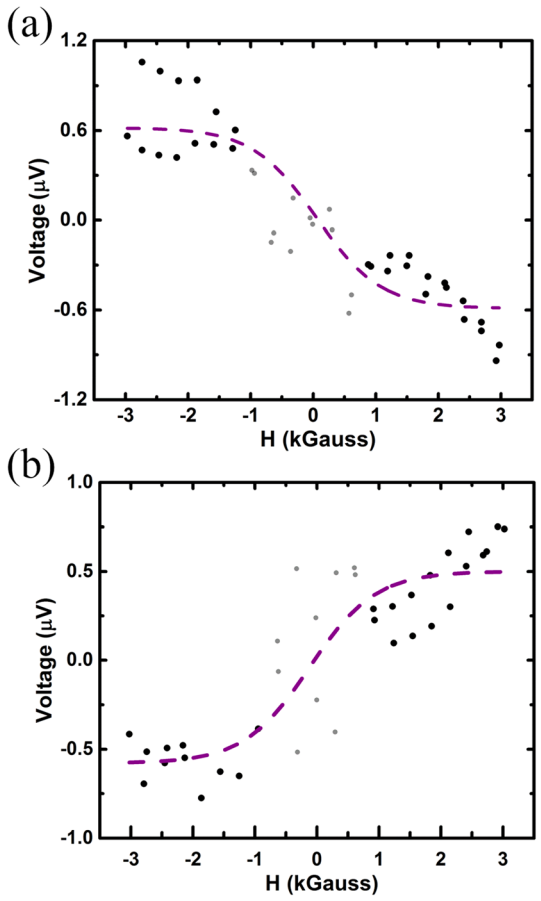

FIG. 5. Inverse spin Hall effect signal. These data were obtained by subtracting out the background contribution from the data presented in Figure 4. The gray data points indicate data that is uncertain due to the large magnetoresistance contribution around −0.5 kG to +0.5 kG. The dashed line shows the anticipated ISHE behavior.

Note that here we have assumed that the devices maintains 100% of its polarization on tunneling from the NiFe into the ZnO. However, the actual I_s may be smaller than 0.7 mA, which makes our calculations here a low-end estimation of the spin-orbit coupling in ZnO. Based on these values, the spin-Hall angle was determined to be approximately 1.6×10^{-2}. Comparing these values to those of silicon, germanium, and platinum, we can see that ZnO has a much larger spin-Hall angle than silicon and germanium (with previously reported spin-Hall angles of approximately 1×10^{-4} and 1×10^{-3}, respectively) and lower than that of platinum (average spin-Hall angle previously reported as approximately 8×10^{-2}).[20,24,25]

To summarize, through these all-electrical investigations, we have shown the potential of ZnO thin films in the realm of spintronic devices. We have shown that, at room temperature, there is a visible ISHE signal, which allows us to accurately quantify the spin-orbit coupling in ZnO. This quantification has shown us that the spin-Hall angle of ZnO is approximately 100 times that of Si and 10 times that of Ge, thereby illustrating its potential over other semiconductors. We believe, through minimal material modifications to ZnO, it should be possible to enhance its ISHE response to a point where it can provide as strong of a signal as Pt. With this strong evidence supporting the use of ZnO in spin detection techniques, it seems only a matter of time before we are able to develop transparent devices capable of coupling the optoelectronic properties of ZnO with its new-found spintronic potential.

The authors thank the US NSF for research support through Grant Nos. 1121252 (MRSEC) and 1234338.

[1]S. J. Pearton, C. R. Abernathy, M. E. Overberg, G. T. Thaler, D. P. Nixon, N. Theodoropoulou, A. F. Hebard, Y. D. Park, F. Ren, J. Kim, and L. A. Boatner, J. Appl. Phys. **93**, 1 (2003).
[2]V. A. Coleman and C. Jagadish, in *Zinc Oxide Bulk, Thin Films, and Nanostructures: Processing, Properties, and Application*, edited by C. Jagadish and S. J. Pearton (Elsevier, Oxford, 2006).
[3]S. Ghosh, V. Sih, W. H. Lau, D. D. Awschalom, S.-Y. Bae, S. Wang, S. Vaidya, and G. Chapline, Appl. Phys. Lett. **86**, 232507 (2005).
[4]D. M. Bagnall, Y. F. Chen, Z. Zhu, T. Yao, S. Koyama, M. Y. Shen, and T. Goto, Appl. Phys. Lett. **70**, 2230 (1997).
[5]H. Nanto, T. Minami, S. Shooji, and S. Takata, J. Appl. Phys. **55**, 1029 (1984).
[6]Z. L. Wang, Appl. Phys. A: Mater. Sci. Process. **88**, 7 (2007).
[7]R. R. Schaller, IEEE Spectrum **34**, 52 (1997).
[8]S. E. Thompson and S. Parthasarathy, Mater. Today **9**, 20 (2006).
[9]L. Risch, Mater. Sci. Eng., C **19**, 363 (2002).
[10]T. N. Jackson, Nature Mater. **4**, 581 (2005).
[11]S. Das Sarma, Am. Sci. **89**, 516 (2001).
[12]M. Johnson, J. Phys. Chem. B **109**, 14278 (2005).
[13]S. A. Wolf, D. D. Awschalom, R. A. Buhrman, J. M. Daughton, S. von Molnár, M. L. Roukes, A. Y. Chtchelkanova, and D. M. Treger, Science **294**, 1488 (2001).
[14]M. C. Prestgard, G. Siegel, Q. Ma, and A. Tiwari, Appl. Phys. Lett. **103**, 102409 (2013).
[15]D. D. Awschalom and M. E. Flatté, Nat. Phys. **3**, 153 (2007).
[16]I. Zutic, J. Fabian, and S. Das Sarma, Rev. Mod. Phys. **76**, 323 (2004).
[17]Y. Gorodetski, A. Niv, V. Kleiner, and E. Hasman, Phys. Rev. Lett. **101**, 043903 (2008).
[18]S. O. Valenzuela and M. Tinkham, Nature **442**, 176 (2006).
[19]K. Uchida, S. Takahashi, K. Harii, J. Ieda, W. Koshibae, K. Ando, S. Maekawa, and E. Saitoh, Nature **455**, 778 (2008).
[20]K. Ando and E. Saitoh, Nat. Commun. **3**, 629 (2012).
[21]J. E. Hirsch, Phys. Rev. Lett. **83**, 1834 (1999).
[22]E. Saitoh, M. Ueda, H. Miyajima, and G. Tatara, Appl. Phys. Lett. **88**, 182509 (2006).
[23]T. Kimura, Y. Otani, T. Sato, S. Takahashi, and S. Maekawa, Phys. Rev. Lett. **98**, 156601 (2007).
[24]M. Koike, E. Shikoh, Y. Ando, T. Shinjo, S. Yamada, K. Hamaya, and M. Shiraishi, Appl. Phys. Express **6**, 023001 (2013).
[25]K. Ando, S. Takahashi, K. Harii, K. Sasage, J. Ieda, S. Maekawa, and E. Saitoh, Phys. Rev. Lett. **101**, 036601 (2008).